

Inkjet Printing of Growth Factor Concentration Gradients and Combinatorial Arrays Immobilized on Biologically-Relevant Substrates[§]

Eric D. Miller^{1,2,3}, Julie A. Phillippi^{2,4}, Gregory W. Fisher², Phil G. Campbell^{1,2,3}, Lynn M. Walker⁵ and Lee E. Weiss^{*,3,6}

¹Biomedical Engineering, ²Molecular Biosensor and Imaging Center, ³Institute for Complex Engineered Systems, ⁴Children's Hospital of Pittsburgh of UPMC, ⁵Chemical Engineering, ⁶The Robotics Institute, Carnegie Mellon University, Pittsburgh, Pennsylvania 15213, USA

Abstract: Current methods for engineering immobilized, 'solid-phase' growth factor patterns have not addressed the need for presentation of the growth factors in a biologically-relevant context. We developed an inkjet printing methodology for creating solid-phase patterns of unmodified growth factors on native biological material substrates. We demonstrate this approach by printing gradients of fluorescently labeled bone morphogenetic protein-2 (BMP-2) and insulin-like growth factor-II (IGF-II) bio-inks on fibrin-coated surfaces. Concentration gradients were created by overprinting individual substrate locations using a dilute bio-ink to modulate the surface concentration of deposited growth factor. Persistence studies using fluorescently-labeled BMP-2 verified that the gradients retained their shape for up to 7 days. Desorption experiments performed with ¹²⁵I-BMP-2 and ¹²⁵I-IGF-II were used to quantify the surface concentration of growth factor retained on the substrate for up to 10 days in serum containing media after rinsing of the unbound growth factor. The inkjet method is programmable so the gradient shape can be easily modified as demonstrated by printed linear gradients with varying slopes and exponential gradients. In addition, the versatility of this method enabled combinatorial arrays of multiple growth factors to be created by printing overlapping patterns. The overlapping printing method was used to create a combinatorial square pattern array consisting of various surface concentrations of BMP-2 and fibroblast growth factor-2 (FGF-2). C2C12 myogenic precursor cells were seeded on the arrays and alkaline phosphatase staining was performed to determine the effect of FGF-2 and BMP-2 surface concentration on guiding C2C12 cells towards an osteogenic lineage. These results demonstrate the utility of inkjet printing for creating orthogonal growth factor gradients to investigate how combinations of immobilized growth factors influence cell fate.

Keywords: Bioprinting, combinatorial arrays, concentration gradients, immobilized growth factors, inkjet printing.

1. INTRODUCTION

We have developed an inkjet printing methodology capable of creating concentration-modulated patterns of growth factors on native substrates including fibrin-coated glass coverslips [1, 2]. The growth factors are immobilized to the fibrin substrate *via* native binding affinity. Our use of the term "native binding affinity" refers to the innate ability of the growth factor to be retained on the fibrin surface without the need for covalent cross-linking or chemical modification. The printing system is programmable, which allows for rapid and simple pattern creation and modification. The surface concentrations of the printed patterns are modulated by overprinting individual substrate locations using a dilute bio-ink. The versatility of this approach permits the rapid creation of patterns with spatially varied and well-defined surface concentrations of growth factor.

We have previously demonstrated that this methodology can be used to reproducibly create immobilized patterns of fibroblast growth factor-2 (FGF-2) on fibrin-coated glass

coverslips, including gradients that modulate cell proliferation in register with the varying surface concentration of growth factor [1, 2]. FGF-2 not only binds heparin [3] but has been shown to contain high affinity binding domains for fibrinogen and fibrin [4, 5]. Recently, we demonstrated that bone morphogenetic protein-2 (BMP-2), which has also been shown to bind heparin [6] can be used with this patterning technique. BMP-2 was printed on fibrin to guide primary muscle-derived adult stem cells from mice towards an osteogenic lineage [7, 8]. In addition, the BMP-2 printing was used to pattern sub-populations of myogenic and osteogenic cells on the same fibrin-coated chip [7, 8]. In the present study, additional printing with BMP-2 was performed as well as another heparin binding growth factor, insulin-like growth factor-II (IGF-II) [9].

Previous studies have focused on printing square patterns or linear concentration gradients with one slope and consisting of one growth factor. The purpose of this study is to further demonstrate the versatility of this printing methodology by creating immobilized concentration gradients of varying slope and shape, as well as overlapping gradients of multiple factors. To create these more complex patterns, we developed a printing strategy which minimizes the non-printed area in the pattern while permitting sufficient drying time for each deposited drop to maintain pattern resolution. The capability to print overlapping patterns also permits the creation of combinatorial arrays, which can be used to quickly

*Address correspondence to this author at the 3113 Newell Simon Hall, The Robotics Institute, Carnegie Mellon University, 5000 Forbes Ave, Pittsburgh, PA 15213, USA; Tel: 412.268.7657; Fax: 412.268.6436; E-mail: lew@cs.cmu.edu

[§]Previously published under Julie A. Jadlowiec.

probe for growth factor inhibition and synergistic effects on cell behavior in a high-throughput manner. As well as demonstrating the utility of this inkjet printing method for creating patterns of heparin-binding growth factors, we also further characterize the retention of these growth factors on the fibrin surface since the patterning is dependent upon the native binding of the growth factor to the fibrin substrate.

Developing a robust method for creating immobilized growth factor patterns is important for *in vitro* cellular studies in developmental biology as well as for advancing regenerative medicine applications. Spatial patterns of endogenous growth factors, in particular, concentration gradients, play critical roles in directing cell migration, proliferation, and differentiation during embryonic development [10, 11] and wound healing [12-14]. Furthermore, several studies suggest that *in vivo* pattern formation occurs, in part, by growth factor sequestration to the extracellular matrix (ECM) or cell surface resulting in immobilized 'solid-phase' spatial patterns [15-17]. We selected fibrin as the printing substrate for these studies because of its ability to immobilize a variety of growth factors at the wound site [18] and its role as a temporary ECM during wound healing [12, 19].

Many patterning approaches have been developed for creating two-dimensional (2D) immobilized protein patterns. Some of the available protein patterning methods include microcontact printing [20, 21], adsorption from solution using microfluidic devices [22-24], inkjet printing [25-29], aerosol-based precision spraying [30], and various methods of photoimmobilization [31, 32]. However, with all of these reported patterning examples, either the protein was chemically modified to permit immobilization, which may result in an unforeseen attenuation in bioactivity, or the proteins were immobilized onto non-biological substrates. The printing methodology presented here has been designed to enable the study of native growth factor patterns on native biological substrates with a full characterization of deposited and retained protein surface concentration. For our experiments, we have utilized the affinity of the growth factors for the fibrin surfaces to create specific and persistent immobilized growth factor patterns. It was beyond the scope of this paper to determine the binding domains for each growth factor. Since inkjet printing does not rely on a pattern template, it has the added advantages of rapid prototyping, whereby pattern parameters can be changed very quickly, and overlapping gradients of molecules can be created rapidly to control cell behaviors as demonstrated here.

2. MATERIALS AND METHODS

2.1. Preparation of Growth Factor Bio-Inks

To visualize printed patterns, the growth factors were labeled with mono-reactive N-hydroxysuccinimide ester cyanine dyes (synthesized in our laboratory) following established protocols [33]. Recombinant human BMP-2 (R&D Systems, Minneapolis, MN) and recombinant human IGF-II (Austral Biologicals, San Ramon, CA) were labeled with Cyanine 5 (Cy5) and Cyanine 7 (Cy7), respectively. Free dye was separated from the labeled growth factors using 3,000 (IGF-II) and 10,000 (BMP-2) molecular weight cut off centrifugal filter devices (Millipore, Billerica, MA) following the manufacturer's protocol. After purification, the stock solutions were stored at -80°C and were thawed and diluted

1 h before printing. IGF-II bio-inks were diluted in 10 mM sodium phosphate, pH 7.4 while the BMP-2 bio-inks were prepared in 20 mM sodium acetate, pH 3.5. Unlabeled BMP-2 and FGF-2 (Peprotech, Rocky Hill, NJ) were used and were diluted in 10 mM sodium phosphate, pH 7.4 and printed for the cell-based assays.

2.2. Substrates for Printing

Fibrin-coated 18 mm glass coverslips (Electron Microscopy Sciences, Washington, PA) were prepared using a method we have previously described [1]. Briefly, the coverslips were cleaned for 2 h in sulfuric acid with NO-CHROMIX (GODAX Laboratories, Cabin John, MD) followed by extensive rinsing with deionized (DI) water. After drying the slides with nitrogen, the glass surfaces were functionalized with 1% 3-aminopropyltriethoxysilane (Gelest, Inc., Morrisville, PA) in a 95% acetone solution for 10 min. The coverslips were then rinsed with acetone, ethanol, and DI water, and dried at 120°C for 45 min. To form reactive aldehyde groups on the surface, the coverslips were incubated in a 3% glutaraldehyde (Electron Microscopy Sciences, Washington, PA) solution in phosphate buffered saline (PBS), pH 7.4, for 2 h at 37°C. After rinsing the coverslips twice with methanol and 3 times with DI water, the functionalized surfaces were incubated in 0.1 mg/mL human fibrinogen (American Diagnostica, Inc., Stamford, CT) diluted in 10 mM sodium phosphate, pH 7.4 for 18 h at 4°C. After aspirating the excess unbound fibrinogen, the remaining active sites were blocked with 0.3 M glycine (Bio-Rad Laboratories, Hercules, CA), pH 7.4 for 2 h at 4°C followed by 3 PBS rinses. The immobilized fibrinogen was converted into fibrin by incubating the coverslips in 4 U/mL thrombin (Enzyme Research Laboratories, South Bend, IN) diluted in 10 mM sodium phosphate buffer, pH 7.4 with 1 mM calcium chloride at 37°C for 2 h. Finally, the coverslips were rinsed 3 times with PBS. Prior to printing on the substrates, the fibrin-coated coverslips were rinsed three times with sterile DI water and air-dried in a laminar flow hood. Along with printing on the fibrin-coated substrates, patterns were also printed on nitrocellulose coated glass slides (FAST™ slides) (Schleicher and Schuell Bioscience, Dassel, Germany) to verify printing accuracy.

2.3. Growth Factor Patterning

Patterns were printed using a custom inkjet deposition system we developed that is described in detail elsewhere [34]. The system uses a piezoelectric drop-on-demand inkjet printhead with a 30 μm diameter nozzle (MicroFab Technologies, Inc. Plano, TX) (Fig. 1A). To create gradients, multiple layers of uniform rectangular patterns of decreasing lengths were printed on top of each other to modulate the surface concentrations and create the desired gradient shape, as illustrated in Fig. 1B). Each layer was printed using a staggered printing technique to maximize drying time of a printed drop before another drop was deposited next to it. A flexible hose blowing a gentle stream of dried air was also directed on the patterns during printing to aid drying. In the time between printing each layer, during which the jet is not firing, the bio-ink in the tip of the inkjet nozzle begins to concentrate due to solvent drying. Therefore, just prior to printing each layer, the inkjet was fired briefly off to the side of the pattern to refresh the bio-ink in the tip. This ensured

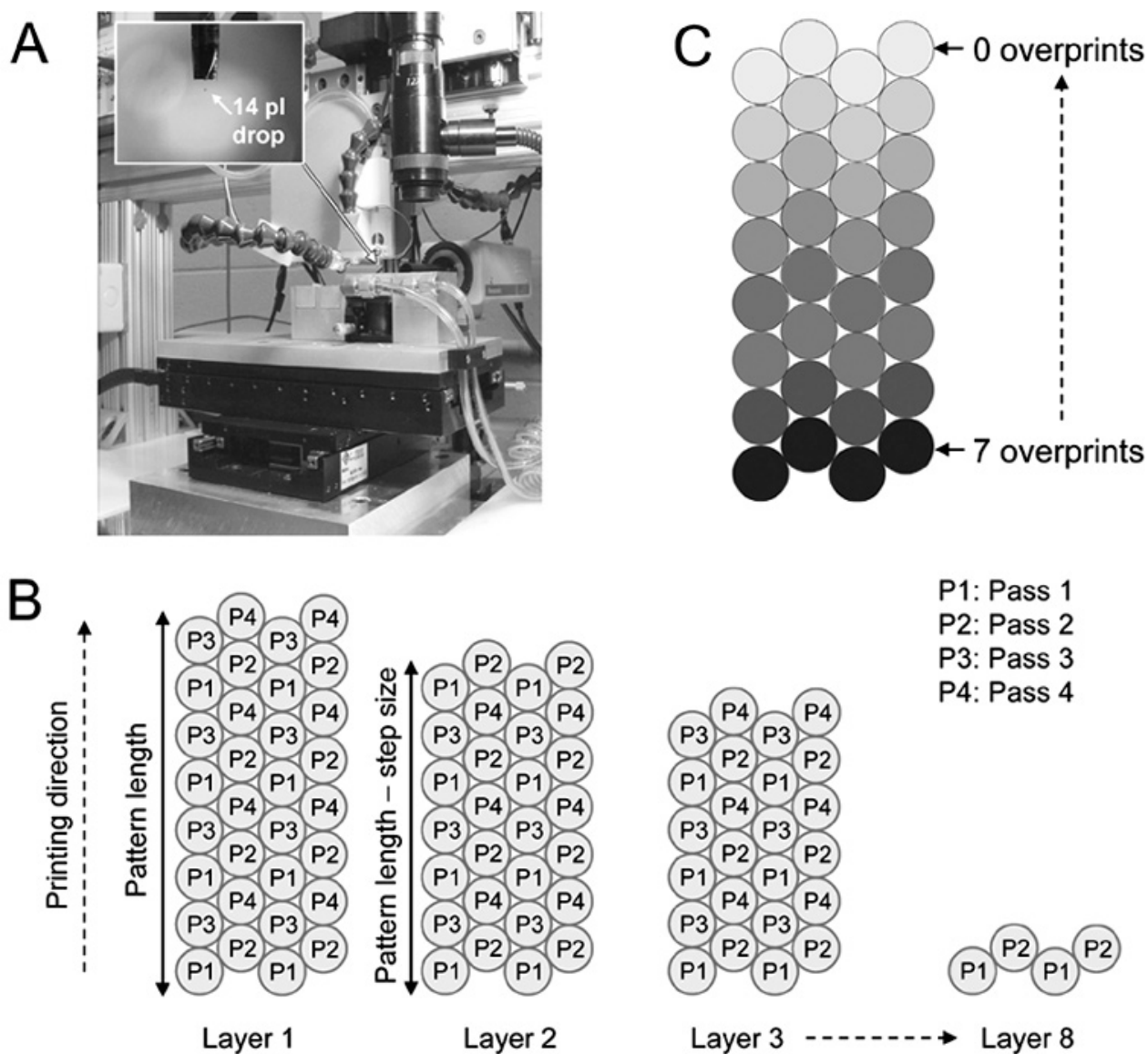


Fig. (1). Inkjet deposition system and overview of gradient printing strategy. **(A)** Custom fabricated 2D inkjet printer: inset, 30 μm diameter nozzle jetting 14 pL drop. **(B)** Illustration of staggered printing strategy for creating individual layers. In this example, the pattern length is decreased by one drop diameter with each successive printed layer, (equivalent to a gradient step size of 67 μm). **(C)** Overprint strategy for creating a linear gradient.

that the first deposited drop in each layer had the same growth factor concentration as subsequent drops in that layer.

Decreasing the pattern length (referred to as the gradient "step size") with each successive printed layer forms a gradient (Fig. 1B, C). The step size concept is further illustrated in Fig. 1(B). For layer 1, each column of the gradient is printed according to a specified pattern length. The pattern length marker shown in Fig. 1(B) is focusing on the first column of the pattern. For layer 2, the printed pattern length is shortened by a specified amount, which we refer to as the gradient step size. For the case shown in Fig. 1(B), the step size is equal to one drop diameter. To achieve a linear gradient, the pattern length was decreased by a fixed step size with each overprint. As the step size is increased, the total number of overprints at the high concentration end of the

gradient becomes lower and the slope of the gradient decreases. Exponential gradients were created by changing the pattern length according to an exponential function during printing. For printing the overlapping gradient patterns with multiple growth factors, the first gradient was printed with one growth factor, the inkjet was then rinsed with water, and the second growth factor bio-ink was loaded into the inkjet. The second pattern was then printed relative to the position of the reference drop recorded in the first pattern. All of the gradients printed were 1.5 mm in length with a center-to-center drop spacing of 67 μm except for the combinatorial arrays which were printed with a drop spacing of 134 μm .

The schematic for printing the combinatorial square arrays is shown in Fig. 2). The FGF-2 bio-ink (10 $\mu\text{g}/\text{mL}$) was loaded first and a 3 (row) x 4 (column) array was printed consisting of 0.75 mm square patterns. The squares were

printed with a 75 μm drop spacing with a distance of 1.75 mm between adjacent squares. For the first row, each square was overprinted 2 times, while the second and third rows consisted of 10 and 20 overprints, respectively. The inkjet was flushed and the BMP-2 bio-ink was loaded (10 μg/mL). With the BMP-2 bio-ink, a 4 x 3 array of squares with the same drop and square spacing as the FGF-2 array was printed so that it partially overlapped with the FGF-2 array. For the BMP-2 array, the first column was overprinted 2 times, and the second and third columns were overprinted 10 and 20 times, respectively. The resultant array contains patterns with different overprints which consist of only one of the bio-inks as well as every combination of overprints for each of the growth factors. After printing, the patterns were rinsed three times with PBS, pH 7.4 to remove unbound growth factor and stored in serum-free Base DMEM (all media components from Invitrogen, Carlsbad, CA) with 1% penicillin/streptomycin (PS) at 4°C until seeded with cells.

2.4. Pattern Imaging and Quantification

Images of cell experiments were acquired with a Leica

DM IRB microscope using a 5X, 0.12 numerical aperture (NA) objective (Leica Microsystems, Bannockburn, IL) and a Retiga 1300 CCD camera (Qimaging, Surrey, BC, Canada) with Northern Eclipse Image Analysis Software (Empix Imaging, North Tonawanda, NY). Printed gradients were imaged using a Zeiss IM35 Axiovert microscope (Carl Zeiss, Inc., Thornwood, NY) equipped with a Photometrics C-250 12-bit cooled CCD camera (Photometrics, Tucson, AZ). The printed coverslips were imaged dry immediately after printing, placed in PBS, pH 7.4 in a 37°C humidified incubator for a minimum of 24 h to allow desorption of unbound growth factor, and the patterns were re-imaged as before. For the gradient persistence experiments, after the 24 h PBS rinse, the patterned coverslips were placed in Opti-MEM® I reduced serum media supplemented with 10% calf serum (CS) and 1% PS and images were taken every 24 h. Images of the gradients consisting of one growth factor and the combinatorial arrays were acquired using a Plan-Neofluar 5X, 0.15 NA objective while images of the overlapping gradients were acquired with a Fluor 2.5X, 0.12 NA objective (both from Carl Zeiss, Thornwood, NY). The fluorescence

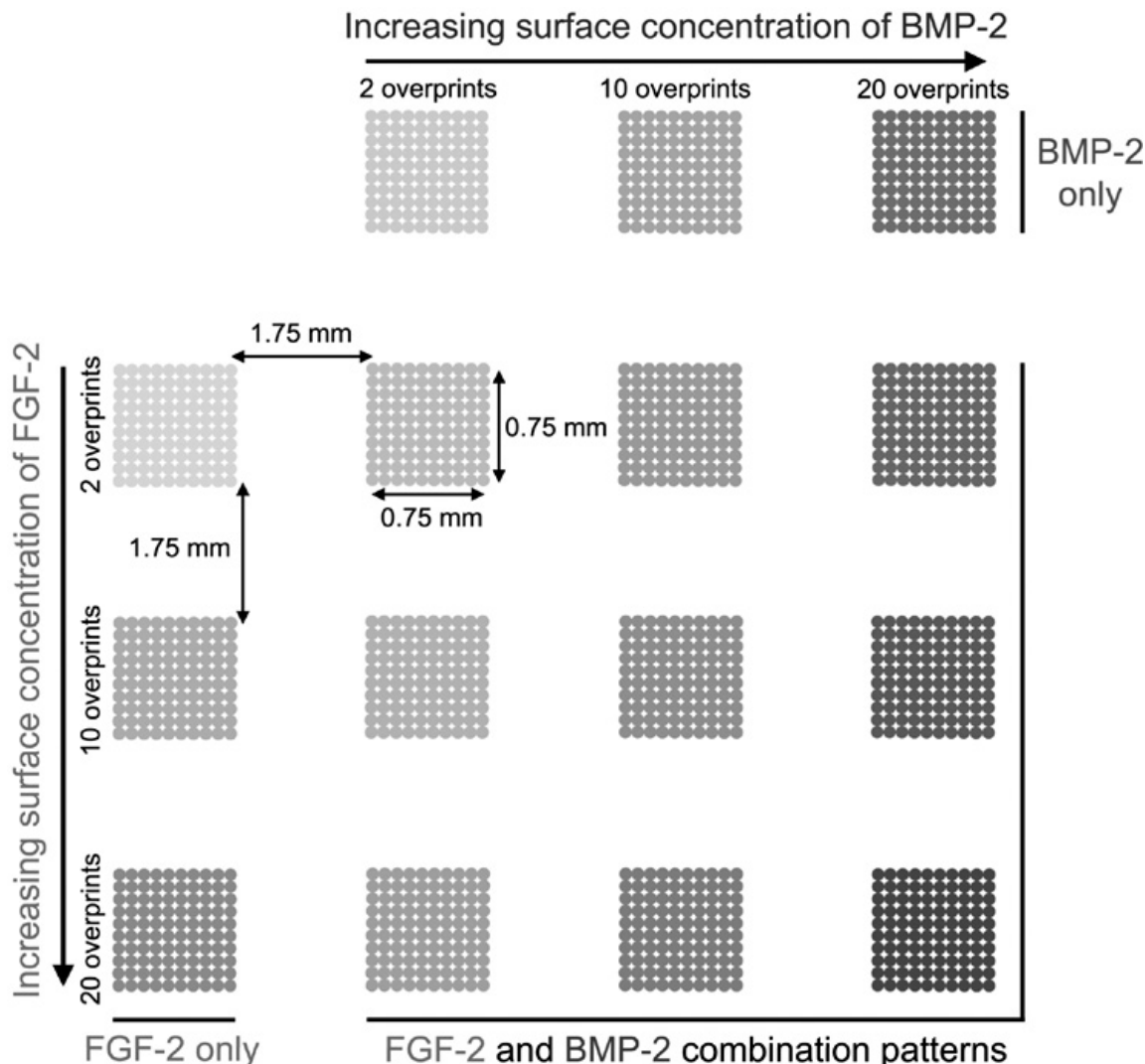


Fig. (2). Schematic for printing combinatorial square array of FGF-2 and BMP-2. Figure not drawn to scale.

filter sets used for imaging were Cy5 (620 excitation:685 emission) and Cy7 (710 excitation:776 emission) (Chroma Technology Corp., Rockingham, VT).

Since the image field was relatively large, image processing was necessary to correct for unevenness in illumination across the field which may adversely affect the “true” shape (linear, exponential) of the gradients being imaged. Consequently, image flatfielding [35] was performed on all gradient images and the background images were inspected to ensure that variation in illumination across the field was faithfully represented. All image processing steps were carried out using the Image Processing Toolbox in MATLAB® version 6.5 (The MathWorks, Inc., Natick, MA). Profiles of the gradients were obtained using ImageJ (v.1.32j) [36]. The pattern area was highlighted and the plot profile tool was used to acquire the average pixel value in each column along the length of the gradient. For the combinatorial arrays, the average pixel value of each drop in the pattern was determined using ImageJ. The drops were averaged across rows to determine the average pixel value of each row of the array for each growth factor.

For the gradient persistence studies, gradient and background images were acquired as described above with only minor changes in the processing protocol. Background images for the first image in the timed sequence were applied to all images in the series for flatfielding and, subsequently, final background levels off-pattern for all images were set to approximately the same level. The same look-up table was then applied to all images in the series for final contrasting. To determine loss of cyanine-labeled growth factor over time, the first two rows of the gradients acquired at each time point were compared for convenience. Each row contained the entire surface concentration range of deposited growth factor. To assess uniformity of fluorescence loss across the pattern, the average pixel value of the first and last drop in the first row of each gradient was determined using ImageJ. These values were used to calculate a relative drop intensity ratio which could be compared across the different time points. This protocol was a useful method for determining persistence of gradient shape. However, a more quantitative method was needed to assess retention of the growth factors on the fibrin surface over time.

2.5. Surface Concentration and Persistence

To quantify the binding and desorption of the growth factors from the fibrin surface, both BMP-2 and IGF-II were iodinated using a chloramine T method [37]. As performed previously [2], the concentrations of the ¹²⁵I-labeled growth factors were selected so that the surface concentrations prepared using the blotting would bracket those that are created during the printing process. The broad range of surface concentrations tested with the ¹²⁵I-labeled growth factors was also useful for determining if saturation of the fibrin surface was achieved during the printing process. A serial dilution of unlabeled growth factor was prepared and the same amount of ¹²⁵I-labeled growth factor was then added to each unlabeled growth factor dilution. Fibrin-coated slides were patterned by placing 1 μ L of the prepared bio-ink on the substrate and allowing it to dry. After determining the quantity of ¹²⁵I-labeled growth factor applied to each slide using a Cobra II auto-gamma counter (Perkin-Elmer, Wellesley,

MA), the slides were rinsed three times in PBS and the amount of ¹²⁵I-labeled growth factor retained was determined again. The slides were then placed in serum free MEM-alpha with 25 mM (4-(2-hydroxyethyl)-1-piperazineethanesulfonic acid) (HEPES), 0.02% sodium azide, and 1% PS and stored at 37°C for 24 h. The radioactive counts were determined again and the serum-free media was replaced with serum containing media. The ¹²⁵I-BMP-2 slides were incubated in MEM-alpha containing 10% CS and the ¹²⁵I-IGF-II slides were incubated in 0.2% CS. These serum concentrations are typical for *in vitro* cell experiments that we perform with each of these growth factors. For *in vitro* experiments with BMP-2, the cells are cultured in medium with 10% CS [8] (also see section 2.6). For proliferation experiments, the cells are cultured in serum-free or reduced serum media [1, 2]. Thus, to simulate *in vitro* culture conditions, the ¹²⁵I-BMP-2 slides were incubated in 10% CS and the ¹²⁵I-IGF-II slides were incubated in 0.2% CS. Radioactive counts were acquired and the media was replaced every 24 h for the first 5 days and at day 7. The final radioactivity measurement was attained at day 10. All retention and surface concentration calculations assumed that the unlabeled growth factor was retained on the fibrin surface in the same manner as the ¹²⁵I-labeled growth factor. All acquired data were corrected to account for radioactive decay.

2.6. Cell Culture and Differentiation Assay

C2C12 myogenic precursor cells were obtained from ATCC (American Type Culture Collection, Manassas, VA) and cultured according to the manufacturer's instructions in growth medium (DMEM (high-glucose), 10% CS, 1% PS) (Invitrogen, Carlsbad, CA). Cells were seeded (approximately 90% confluence) in growth medium onto coverslips containing BMP-2/FGF-2 co-printed patterns and cultured in the presence of 1 μ g/mL aprotinin for 72 h. The cells were then rinsed in PBS and fixed for 2 min in 3.7% formaldehyde. Alkaline phosphatase activity (ALP) was detected using a leukocyte alkaline phosphatase kit (product number 86C from Sigma Chemical Co., St. Louis, MO) according to the manufacturer's instructions.

3. RESULTS

3.1 Gradient Shape

To demonstrate the versatility of our inkjet printing method, linear gradients of varying slope and exponential gradients were printed using Cy5-BMP-2 (Fig. 3). Patterns were printed on both nitrocellulose (row A), an idealized substrate designed for protein binding, and on fibrin-coated coverslips, representing a native biological substrate (rows B and C). The gradients in row B were imaged immediately after printing and the gradients in row C are the same gradients after a 24 h rinse in PBS to remove any unbound growth factor. The bright spots seen on the patterns printed on fibrin are not due to the printing, but are fluorescence artifacts on the fibrin substrate.

Plots of the average pixel value along the length of the gradients are shown in Fig. (4). The drop-off in pixel value at the $x = 0$ mm end of each gradient is due to the offset of adjacent rows in the gradient where the black background is averaged with the brighter printed drops. The plots of the linear patterns on nitrocellulose demonstrate that the printing

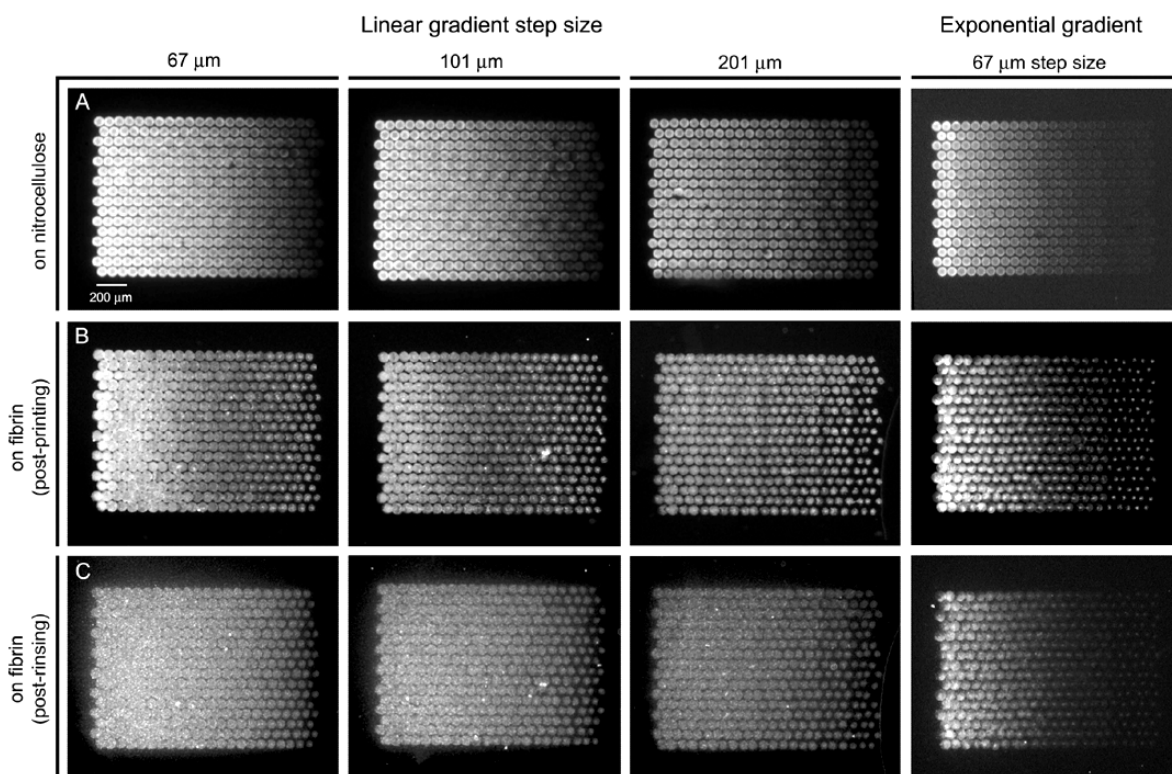


Fig. (3). Gradients with varying shape printed on an idealized and biological substrate. Gradients with different shapes (controlled by varying the gradient step size and overprint strategy) were printed on both nitrocellulose-coated slides and fibrin-coated coverslips. Gradients printed on nitrocellulose are shown in row (A). Cy5-BMP-2 bio-inks were used to print the gradients (80 $\mu\text{g}/\text{mL}$ for the linear and 10 $\mu\text{g}/\text{mL}$ for the exponential gradients). The same gradients printed on fibrin substrates before any rinsing are shown in row (B). A lower concentration of Cy5-BMP-2 was used for the linear gradients (40 $\mu\text{g}/\text{mL}$) on fibrin, but the same concentration was used for the exponential gradient (10 $\mu\text{g}/\text{mL}$). The gradients on fibrin after a 24 h rinse in PBS are shown in row (C). The gradients in the first column were all created with a 67 μm step size between overprints while the gradients in the second and third columns were printed with a 101 μm and a 201 μm step size, respectively. The gradients in the fourth column were printed with a 67 μm step size but the pattern length was decreased as an exponential rather than a linear function along the length of the gradient during printing.

can be used to create linear concentration gradients with varying slope (row 1, left column) and that the gradient becomes steeper as the gradient step size is decreased. The plots of the linear patterns on fibrin immediately after printing (row 2), using the same code as those printed on nitrocellulose, indicate that the gradients do not appear to be as linear on fibrin. After incubating the same patterns in PBS to rinse away any unbound growth factor, the gradient shape became more linear (row 3). The shape of the exponential gradient was the same on nitrocellulose and on fibrin post-printing (right column). After rinsing, the exponential shape was maintained on the fibrin with a slight change in the magnitude of the spatial decay.

3.2. Pattern Retention and Surface Concentration Determination

Since the growth factors are being printed onto a biological surface with a limited number of growth factor binding sites and are bound *via* native affinity, it is important to characterize persistence of pattern shape and to quantify the surface concentration of growth factor retained over time. To examine persistence of the shape of the gradients printed on the fibrin surface, printed patterns of Cy5-BMP-2 were placed in serum-containing medium and imaged every 24 h.

The images of the gradients at different time points were normalized so that the pattern profiles could be compared directly to assess gradient shape and magnitude over time (Fig. 5A-C). The gradient was printed using a 40 $\mu\text{g}/\text{mL}$ Cy5-BMP-2 bio-ink with a 201 μm step size. Fig. (5B) is a plot profile of the gradients in Fig. (5A); averaging in the x-direction over each. The lines shown for each of the time points are regression lines fitted across the entire length of the gradient profile. Despite the shift in the fitted line to lower values over time, the overall shape of the gradient is maintained after 7 days. To determine if the fluorescence intensity at the low and high end of the gradient was being lost at the same rate, the relative drop in intensity (I_2/I_1) was calculated for each of the time points (Fig. 5C). Within the standard deviation of the average pixel values of the drops, the ratios indicate that the loss in intensity is approximately equal for each of the time points indicating a uniform loss of fluorescence across the pattern over time.

To better quantify the binding characteristics of the growth factors from the fibrin surface, desorption experiments were performed using ^{125}I -labeled BMP-2 and IGF-II mixed with unlabeled growth factor. Five different surface concentrations of BMP-2 and four different surface concen-

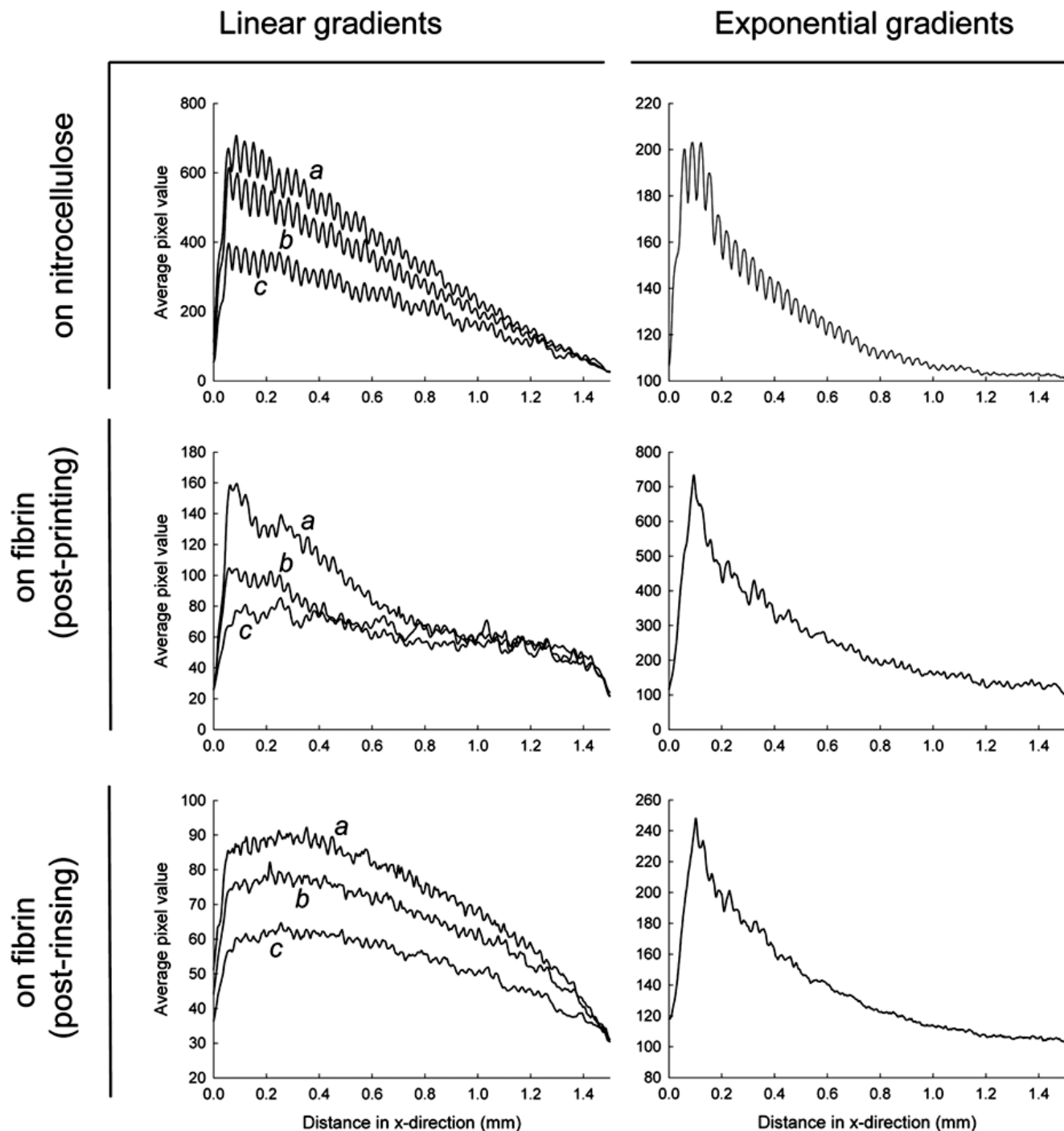


Fig. (4). Quantifying gradient shape. The average pixel value along the length of each of the gradients was determined from the fluorescence images of the gradients in Fig. (3). The left column consists of the profiles of the linear gradients with different slopes while the right column contains the plots for the exponential gradients. The different substrates and conditions are presented in each row: on nitrocellulose (row 1), on fibrin prior to rinsing (row 2), and on fibrin post-PBS rinse (row 3). For the plots with the linear gradients: 67 μm step size (a); 101 μm (b); 201 μm (c).

trations of IGF-II were applied to the fibrin coated substrates to represent the range of growth factor surface concentrations applied when printing. The slides were rinsed three times in PBS followed by an overnight incubation in serum-free media to remove unbound growth factor and were then placed in serum-containing medium. The desorption profiles

for BMP-2 and IGF-II are shown in Fig. (6A, B), respectively (highest surface concentration for BMP-2 not shown). The time zero point indicates the surface concentration of BMP-2 and IGF-II after the three rinses in PBS prior to the 24 h incubation in serum-free media. As seen in each of the curves in Fig. (6A, B), there is an initial loss of adsorbed

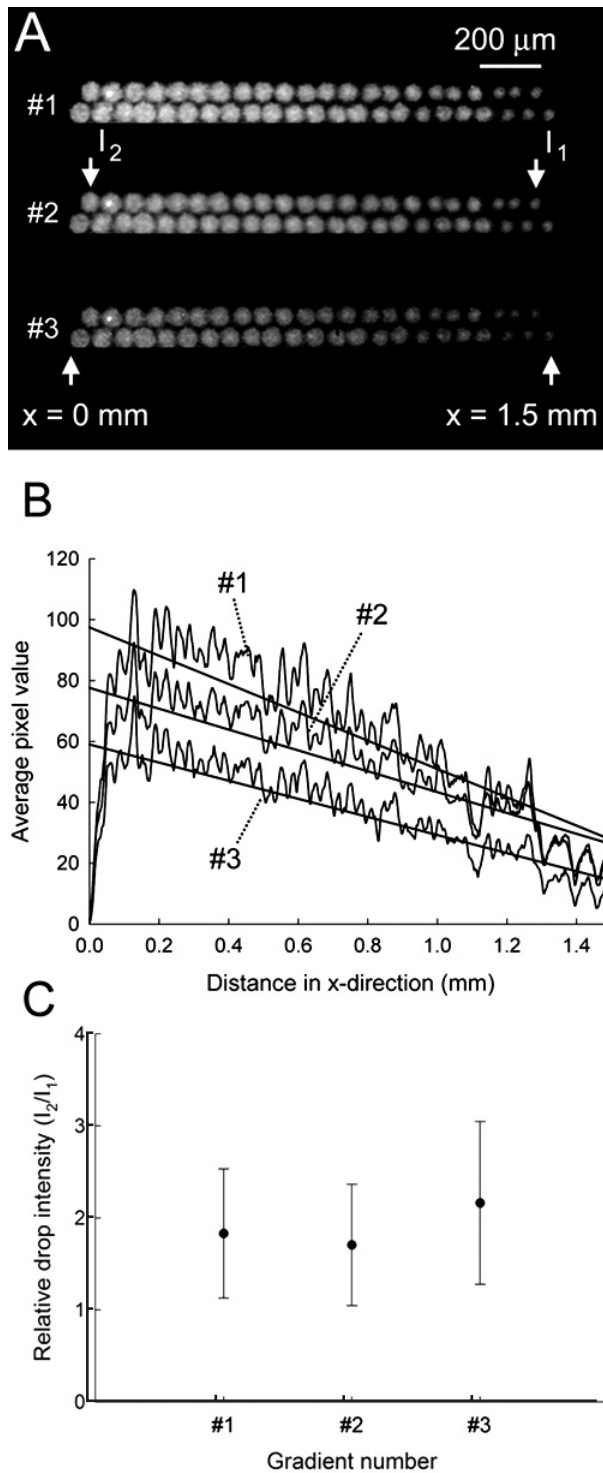


Fig. (5). Persistence of gradient shape over time. **(A)** The first two rows of a gradient printed on fibrin with a 40 $\mu\text{g}/\text{ml}$ Cy5-BMP-2 bio-ink with a 201 μm step size imaged after 46 (#1), 90 (#2), and 168 (#3) hours. **(B)** The average pixel value along the length of each gradient section in the x-direction, and the lines for each of the profiles are regression lines fitted across the entire profile of the gradient. **(C)** The average pixel value of the first (I_2) and last (I_1) drop in the first row of each gradient was used to calculate a relative drop intensity. The error bars represent \pm SD of the average pixel value of the drops.

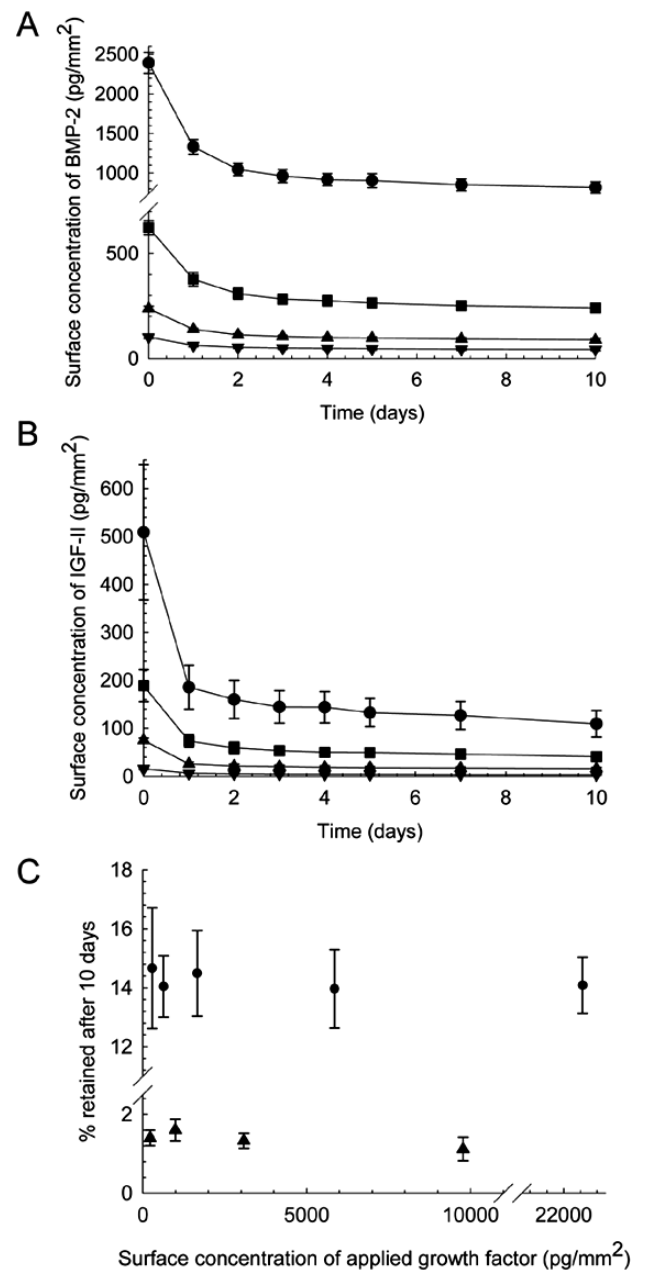


Fig. (6). Desorption profiles and retention of BMP-2 and IGF-II from fibrin-coated printing substrates determined using ¹²⁵I – labeling. Four different surface concentrations were initially applied. **(A)** For BMP-2: 290 \pm 19 pg/mm^2 ▼, 633 \pm 21 pg/mm^2 ▲, 1662 \pm 66 pg/mm^2 ■, 5850 \pm 222 pg/mm^2 ●. **(B)** For IGF-II: 227 \pm 20 pg/mm^2 ▼, 995 \pm 48 pg/mm^2 ▲, 3083 \pm 84 pg/mm^2 ■, 9774 \pm 881 pg/mm^2 ●. Time zero represents the growth factor surface concentration after 3 rinses in PBS. **(C)** The surface concentration of applied growth factor and corresponding percentage of growth factor retained on the fibrin surface after 10 days in media: BMP-2 (●); IGF-II (▲). Each point represents mean \pm SEM of three different experiments.

growth factor in the first 24 h in serum-free media. There is an additional loss after the second 24 h interval in serum-containing media, after which, the surface concentration re-

mains nearly constant indicating little additional loss. In a typical experiment, cells are seeded on the slides after the unbound growth factor has been removed which is shown as day 2 in Fig. (6A, B). Table 1 illustrates the surface concentration of growth factor applied to the surface, the amount retained after the three PBS rinses and 24 h in serum-free media, after 24 h in serum media, and the amount retained after 10 days in culture. After the PBS rinses and the 24 h incubation in serum-free media (data points at Day 1 (Fig. 6A, B)), $22 \pm 3\%$ of the applied BMP-2 is retained while only $2.4 \pm 0.8\%$ of the applied IGF-II is retained. There is an additional loss after the initial 24 h incubation in serum media (data points at Day 2 in Fig. (6A, B)). However, of the BMP-2 and IGF-II remaining after the initial incubation in serum-free media (data points at Day 1, Fig. (6A, B)), approximately 80% was retained after the initial 24 h incubation in serum media (data points at Day 2, Fig. (6A, B)). Approximately 80% of the BMP-2 and 70% of the IGF-II remaining after the initial incubation in serum media (data points at Day 2 in Fig. (6A, B)) is retained for the next 8 days in serum media (data points at Day 10 in Fig. (6A, B)). This experiment demonstrates the most rigorous conditions for the patterns where serum proteins are present to displace the growth factors from the fibrin surface and the media is changed daily. However, even in these extreme conditions, a portion of the applied growth factor is retained as demonstrated in Fig. (6C). Regardless of the surface concentration created on the substrate, the amount retained is consistent for both BMP-2 and IGF-II with a drastic difference in binding between the growth factors. The BMP-2 retention is approximately 14% while IGF-II is less than 2% suggesting that BMP-2 has a higher affinity for fibrin than IGF-II. This figure also demonstrates that the surface concentrations applied to the substrate during the printing are below the saturation level of the substrate since the percentage retained is constant for the surface concentrations examined.

By determining the amount of growth factor retained on the fibrin surface, the surface concentration range as well as the slope of the gradients created in Fig. (3) can be determined. These calculations are given in Table 2. As demonstrated by the plots of the fluorescence intensity of the gradients (Fig. 3), the surface concentration at the high end of the gradient decreases as the step size is increased. The BMP-2 gradients printed here have a retained surface concentration of 18 pg/mm^2 at the low end of the gradient and the retained concentration at the high end is 390, 266, and 124 pg/mm^2 for a step size of 67, 101, and $201 \text{ }\mu\text{m}$, respectively.

3.3. Overlapping Gradients and Combinatorial Arrays with Multiple Growth Factors

The versatility of this inkjet printing methodology also allows for overlapping gradients of multiple growth factors to be patterned as demonstrated in Fig. (7). In Fig. (7A), the gradients were printed on fibrin with the Cy5-BMP-2 bio-ink deposited first (red) followed by the Cy7-IGF-II bio-ink (green). In the example shown in Fig. (7A), opposing gradients with a $134 \text{ }\mu\text{m}$ step size were printed with overlap of the two gradients in the middle portion (0.75 mm) of the pattern. A plot of the average pixel value in the x-direction for the opposing IGF-II and BMP-2 gradients (Fig. 7B) demonstrates that the linear shapes of the gradients are maintained despite printing multiple layers of growth factors directly on top of each other. The plot profiles of the individual and overlapping regions were very similar and, consequently, the individual profiles for each region are not shown. Instead, profiles consisting of the individual as well as the overlapping region of the gradient were obtained as indicated by the colored brackets in Fig. (7A).

The strategy for printing overlapping gradients can also be easily altered to make combinatorial arrays of multiple growth factors by printing gradients with a 90° rotational offset and increasing the drop spacing as shown in Fig. (7C).

Table 1. Surface Concentration of BMP-2 and IGF-II Applied to Fibrin-Coated Surface, Amount Retained After 3 PBS Rinses and 24 h in Serum-Free Media, Amount Retained After 24 h in Serum-Containing Media, and Amount Retained After 10 Days

Applied BMP-2 Surface Concentration (pg/mm^2)	BMP-2 Surface Concentration After 3 PBS Rinses and 24 h Serum-Free Media Incubation (pg/mm^2)	BMP-2 Surface Concentration After 24 h 10% Serum Media Incubation (pg/mm^2)	Final BMP-2 Surface Concentration (pg/mm^2)
22450 ± 825	5201 ± 312	4078 ± 194	3162 ± 180
5850 ± 222	1331 ± 94	1045 ± 77	817 ± 71
1662 ± 66	377 ± 33	309 ± 27	241 ± 22
633 ± 21	139 ± 4	113 ± 6	89 ± 6
290 ± 19	62 ± 7	53 ± 6	43 ± 5
Applied IGF-II Surface Concentration (pg/mm^2)	IGF-II Surface Concentration After 3 PBS Rinses and 24 h Serum-Free Media Incubation (pg/mm^2)	IGF-II Surface Concentration After 24 h 0.2% Serum Media Incubation (pg/mm^2)	Final IGF-II Surface Concentration (pg/mm^2)
9774 ± 881	186 ± 46	160 ± 40	109 ± 28
3083 ± 84	74 ± 13	59 ± 12	41 ± 6
995 ± 48	26 ± 4	21 ± 4	16 ± 3
227 ± 20	6 ± 0.5	5 ± 0.6	3 ± 0.4

Data were obtained from ^{125}I -labeling of BMP-2 and IGF-II. Results represent mean \pm SEM of three different experiments.

This 12 by 12 element array, which consists of printed drops with a drop spacing of 134 μm , represents a two-way combination of the growth factors. The array was created by first printing a gradient using a Cy5-BMP-2 bio-ink (red), followed by a gradient printed using a Cy7-IGF-II bio-ink (green) with a 90° offset to the BMP-2 array. The corresponding plot of the average pixel values of the drops shown in Fig. (7D) demonstrates that the BMP-2 and IGF-II gradients are both maintained. The size of the array is not limited to 144 elements as shown here, but is scalable to probe a larger number of growth factor combinations.

Table 2. Gradient Step Size and Corresponding Surface Concentration Range and Slope

Gradient Step Size (μm)	Retained Surface Concentration Range (pg/mm^2)	Slope of Gradient ($\text{pg}/\text{mm}^2 \cdot \text{mm}$)
67	18-390	248
101	18-266	165
201	18-124	71

3.4. C2C12 Response to Combinatorial Square Arrays of BMP-2 and FGF-2

To demonstrate a biological application for overprinting with multiple growth factors, a 3×4 array of FGF-2 squares ($10 \mu\text{g}/\text{mL}$ bio-ink) was printed first and a 4×3 array of BMP-2 squares ($10 \mu\text{g}/\text{mL}$ bio-ink) was then printed to overlap with some of the FGF-2 squares to create a combinatorial array (Fig. 2). C2C12 precursor cells were seeded on the slides and after 72 h the cells were fixed and stained for ALP expression (Fig. 8). On the printed patterns of BMP-2 alone, there was a dose-dependent increase in ALP expression in register with the printed patterns. In the control field (no pattern) and on the FGF-2 patterns alone, there was no noticeable expression of ALP. For the combination patterns, as the surface concentration of FGF-2 increased, the expression of ALP generally decreased on the BMP-2 patterns. Minimal, yet detectable ALP expression was observed with the $64 \text{ pg}/\text{mm}^2$ BMP-2 column. Increasing the surface concentrations of FGF-2 resulted in no detectable level of ALP expression. The same general trend of decreasing ALP staining in register with increased FGF-2 surface concentration was also observed with the $320 \text{ pg}/\text{mm}^2$ and $640 \text{ pg}/\text{mm}^2$ BMP-2 columns despite the limited sensitivity of the colorimetric

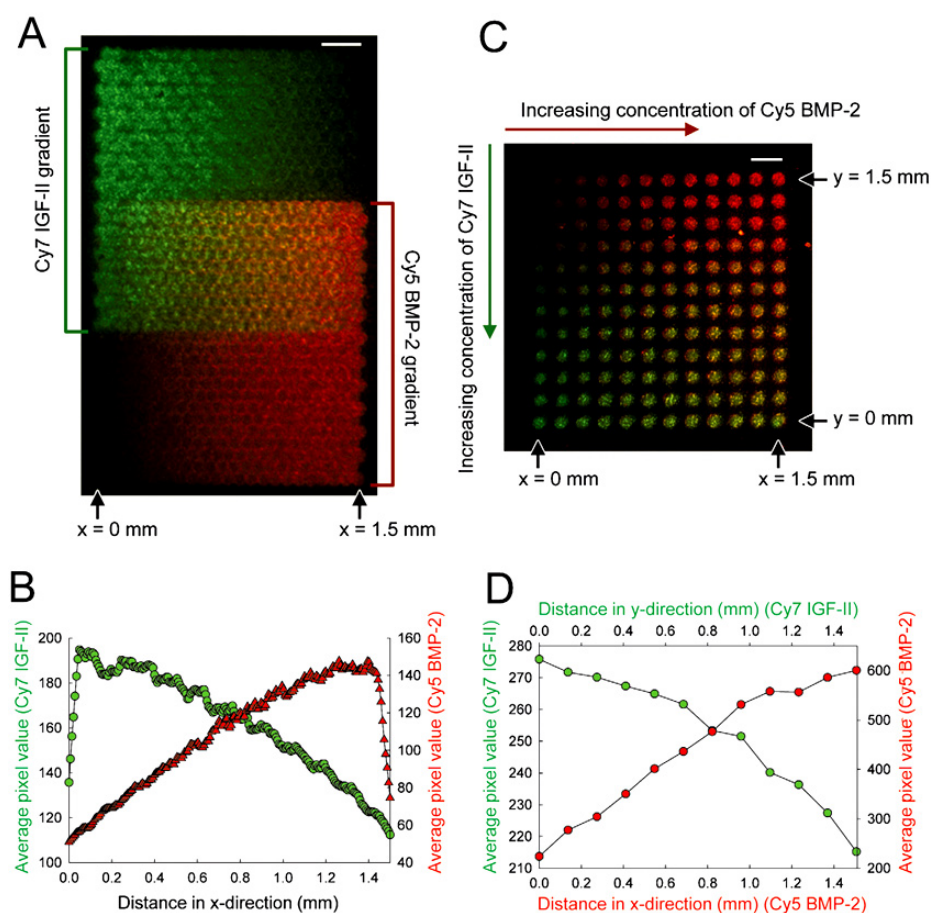


Fig. (7). Printing overlapping gradients and combinatorial arrays with multiple growth factors. (A) Opposing gradients were printed on fibrin using a $40 \mu\text{g}/\text{mL}$ Cy5-BMP-2 bio-ink (red) followed by a $40 \mu\text{g}/\text{mL}$ Cy7-IGF-II bio-ink (green) with a 0.75 mm section of overlap. The average pixel value along the length of the pattern for the individual growth factors is shown below (B). The plot profile for each growth factor was obtained using the entire width of the pattern, including the overlapping portion of the gradient as indicated by the colored brackets. (C) Combinatorial array consisting of 90° offset gradients of BMP-2 ($40 \mu\text{g}/\text{mL}$ bio-ink) and IGF-II ($40 \mu\text{g}/\text{mL}$ bio-ink) and the corresponding plot profile in x (BMP-2) and y (IGF-II) (D). Scale bars represent $200 \mu\text{m}$.

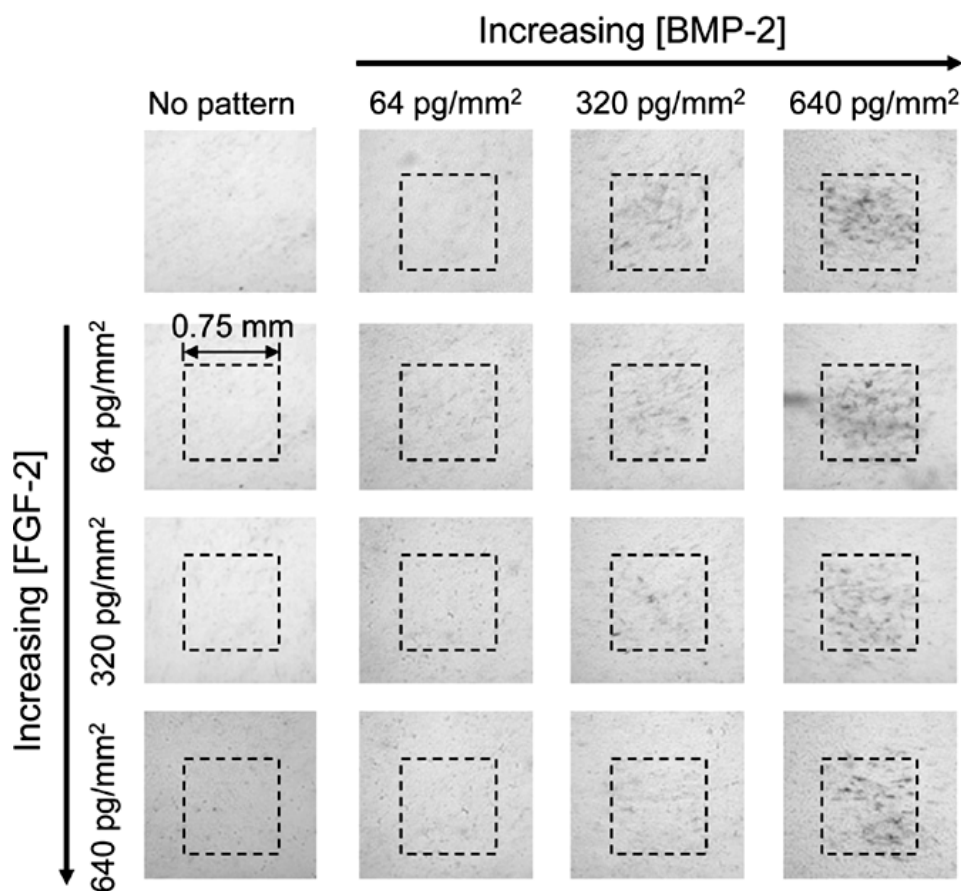


Fig. (8). Printing overlapping square patterns to create a combinatorial array of BMP-2 and FGF-2 that directs cell fate. A 3 x 4 square array using a 10 $\mu\text{g/mL}$ FGF-2 bio-ink was printed on the fibrin substrate first followed by a 4 x 3 array of BMP-2 using a 10 $\mu\text{g/mL}$ bio-ink. The top left image is a control field with no printed pattern. The top row consists of patterns printed with BMP-2 only and the first column consists of patterns printed with only FGF-2. The other squares in the array consist of a combination of FGF-2 and BMP-2. The surface concentrations indicated for each row (FGF-2) and column (BMP-2) are the surface concentrations of each growth factor that were applied during patterning. The dashed square boxes indicate the location of the printed squares. C2C12 myogenic precursor cells were seeded on the patterns at approximately 90% confluence and cultured in growth medium on the substrate for 72 h. The cells were then fixed and stained for alkaline phosphatase activity.

assay used. Experiments were also performed where the BMP-2 was printed first and then FGF-2 with the same results observed.

4. DISCUSSION

Printing onto nitrocellulose substrates, which are idealized substrates engineered for protein binding, was used to verify the accuracy of the printing code and to serve as a reference to compare with printing on fibrin. The appearance of the printed drops on each of the substrates was dramatically different. The drops on the nitrocellulose had a bright outer ring and a dark center while the printed drops on the fibrin generally appeared more homogeneous (Fig. 3). This “coffee-ring” observed when printing on the nitrocellulose is a well described phenomenon [38] and occurs on surfaces where contact line pinning occurs. Drops printed on the nitrocellulose also appeared discrete with very little blending between adjacent drops while the drops printed on the fibrin appeared to spread and blend more. This effect is likely due to the nature of the substrates since the nitrocellulose does not wet as well as the fibrin surface. The spreading and

blending of the drops was reflected in the profiles of the gradients (Fig. 4). For the gradients printed on nitrocellulose, peaks and troughs were observed in the plot profile of each gradient because the drops are discrete whereas on the fibrin substrates, the gradient shapes were smoother. The smoothing of the gradients printed on fibrin after rinsing (Fig. 3, row C) may be due to local diffusion from the individual printed drops followed by readsorption of the growth factor into the area immediately surrounding the drops. When compared to immobilized gradients formed using microfluidics [22-24], the patterns presented here do not appear continuous or smooth. This is partially due to the inkjet printing approach as well as the inhomogeneity of the underlying substrate. The patterns that we create are made up of approximately 70 μm spots and the gradient was formed by changing the spot size which is limited by the diameter of a printed spot. This results in a gradient with a step change in concentration on the order of a drop diameter as opposed to being continuous. However, the advantage of this technique is being able to deposit a known amount of protein at a precise location which allows well-characterized patterns of

almost any desired shape to be made quickly. In addition, focused spraying and higher resolution inkjet printing of biological molecules is feasible for creating spots with diameters of 25-30 μm [30, 39]. This resolution is still well below the sub-micron patterns that can be created with photolithography, however, the current printing resolution is sufficient for influencing cell populations [1, 2]. Unlike many of the idealized printing substrates, the printing surface used here is not perfectly homogeneous since the fibrin layer is formed by protein adsorption which may result in localized areas of the substrate where there is more bound fibrin and, as a result, more growth factor upon printing. However, the discrete and step-like appearance of the printed gradients does not seem to adversely affect the activity of the printed patterns as demonstrated by the cellular response to these gradients [1].

The altered shape of the linear gradients on fibrin immediately after printing (Fig. 4), in comparison to the linear gradients printed on nitrocellulose using the same printing programs, can also be attributed to the substrate. The nitrocellulose coating is 11 μm thick while the fibrin coating is approximately 20 nm thick [1]. Because of this thickness difference, the nitrocellulose wicks water while the fibrin surface does not. When printing on the fibrin surfaces, each deposited drop must be totally dry before another drop is printed next to it or the drops will merge and puddling may occur. This is reflected in the plot profile of the linear gradients on fibrin post-printing (Fig. 4). Between $x = 0$ and 0.5 mm, there is a large plateau at the highest concentration end of each gradient where puddling occurred. Drop merging did not cause any distortion of the exponential gradient shape because less liquid was deposited on the fibrin surface which permitted the deposited drops to dry fully. For these reasons, the staggered printing strategy employed here along with the stream of dry air directed on the patterns during printing was designed to minimize drop merging and puddling, however, it was not totally eliminated.

Fortunately, since a biological printing substrate is used where desorption of the growth factor from the surface is going to occur, the distortions in the linear patterns printed on fibrin due to the puddling were lost after the unbound growth factor desorbed, resulting in a pattern that appeared closer to linear (Fig. 4). The plateau at the high concentration end of each gradient is where puddling occurred resulting in a loss of the gradient shape. For the exponential gradient, the profile maintained its exponential shape after rinsing. However, if the exponential gradient was not printed with a steep enough decay, then the pattern, after rinsing, appears linear as well (data not shown). While the fibrin-coated substrates are not an ideal surface for protein patterning because of their lower capacity for protein binding and their wetting properties, these surfaces are more relevant for conducting biological experiments since they provide a suitable substrate for cell attachment and movement and present the growth factors in a biologically-relevant context. In addition, as demonstrated in this study, the fibrin surface is sufficient for maintaining the resolution and retention of these growth factor patterns.

When printing a new growth factor, several key characterization experiments must be performed as demonstrated here. First, the persistence and retention of the growth fac-

tors on the printing surface over time must be evaluated. We chose to determine persistence of gradient shape by acquiring images of the gradients over 7 days and normalizing the images so that the gradients could be compared directly. This provided a qualitative indication of desorption, however, this method was not totally reliable because photobleaching may occur since 30 sec exposures were required to image the patterns. The plot profiles and the relative drop intensity calculations indicated that the loss in fluorescence intensity was uniform across the pattern, thus indicating that photobleaching was partially responsible for the loss over time. Despite this loss, the gradients maintained their shapes for up to 7 days relying on the native binding of the growth factor to the fibrin.

To overcome the limitations of fluorescence, the binding properties of the growth factors on the fibrin surface were also determined using radioactivity. Characterization and quantification of the binding properties of the growth factor to the printing substrate is essential for designing proper *in vitro* studies and to verify that the surface concentration applied is below saturation since fibrin has a limited number of binding sites. By determining the retention of the growth factors on the fibrin surface over time, the patterns can be rinsed sufficiently prior to cell seeding so that the cells are interacting with immobilized growth factors and not responding to primarily chemotactic gradients caused by soluble growth factors. For FGF-2, three rinses in PBS and an overnight incubation in serum-free media were sufficient to remove all of the unbound growth factor [2]. As a result of the experiments performed here with ^{125}I -labeled growth factors, patterns printed with BMP-2 and IGF-II will need to be incubated an additional 24 h in serum containing media to remove the unbound growth factor.

Retention experiments were performed with both BMP-2 and IGF-II individually. However, growth factor retention may be significantly altered when printing overlapping patterns consisting of multiple growth factors. Additional experiments need to be performed to determine how growth factor retention is affected by the order of the printing or by the different affinities of the growth factors for the substrate. Based on the results presented in this manuscript, the order of printing does not seem to affect the cell response. The combinatorial arrays in Fig. (8) were created by printing FGF-2 first followed by BMP-2 and also the reverse with BMP-2 followed by FGF-2 with similar cell responses observed for each. This result demonstrates that despite printing the second growth factor directly on top of the first, both growth factors were accessible to the cell and the combination of growth factors dictated the cell fate.

When determining what types of growth factors can be used with this technique, we have found that the ideal candidates contain heparin binding domains or domains that are specific for binding fibrin. All of the growth factors that we have successfully printed, including IGF-II and BMP-2 in this study, FGF-2 in this and prior studies [1, 2], and platelet-derived growth factor-BB (PDGF-BB), heparin-binding epidermal growth factor, and hepatocyte growth factor (data not shown) contain heparin binding domains [3, 6, 9, 40-42] with FGF-2 binding fibrin as well [4, 5]. The retention of the growth factor on the fibrin surface correlates with the affinity of the growth factors for heparin. For example, FGF-2

has a higher affinity for heparin than PDGF-BB [3]. When the same amounts of each growth factor are printed, we observe higher retention and thus an increased biological response with FGF-2 compared to PDGF-BB (data not shown). The use of heparin binding proteins is not a limitation to this methodology since many proteins have a native affinity for heparin [43], or can be engineered with a heparin binding domain, such as insulin-like growth factor-I [44]. In addition to printing a variety of growth factors, the printing substrate can be modified as well to contain a variety of ECM proteins. For example, surfaces containing mixtures of fibrin, fibronectin, and collagen I can easily be created to determine what role the ECM content plays in modulating the cellular response to specific growth factors. Creating hybrid surfaces may also increase the binding affinity for some of the growth factors since IGF-II has been shown to bind to vitronectin [45].

The overlapping gradients and combinatorial arrays shown in Figs. (7, 8) were created to demonstrate that this printing method could be used to investigate how growth factor combinations can guide cell fate. The biological example demonstrated here was a combinatorial array consisting of BMP-2 and FGF-2 squares. Growth factors are traditionally delivered *in vitro* to cells as soluble factors, a method referred to as 'liquid-phase' delivery. When delivered in the liquid-phase, BMP-2 has been shown to cause increased ALP activity and osteocalcin production in C2C12 precursor cells, thus directing them towards an osteoblastic lineage [46]. In addition, our group has used immobilized patterns of BMP-2 to direct the fate of mouse muscle-derived stem cells towards an osteogenic lineage [7, 8]. FGF-2 has been shown to inhibit BMP-2 directed osteoblastic differentiation and decrease ALP expression when both growth factors are delivered *via* liquid-phase delivery [47] and, in our lab, when the BMP-2 is immobilized and FGF-2 is present in the medium [8]. A direct comparison between liquid-phase and solid-phase growth factor concentrations cannot be performed because the two delivery methods are not equivalent. For the experiment shown in this manuscript, (Fig. 8), both growth factors are immobilized in a combinatorial array format so that the influence of multiple FGF-2 surface concentrations on BMP-2 stimulated osteogenic differentiation can be determined simultaneously in one experiment on a single chip.

In addition to the ease of programming different patterns, the actual printing is relatively rapid. The gradients shown in Fig. (3) required less than 10 min to print, and the overlapping gradients in Fig. (7) required approximately 30 min (25 min to print, 5 min to switch bio-inks). The delay of switching bio-inks could be easily removed with the addition of multiple print heads. Small working volumes of bio-ink can be used for printing with 30 μ L being sufficient to load the inkjet and print patterns continuously for more than 4 h (at 14 pL/drop, approximately 3 μ L are jetted in 4 h). As well as the speed with which patterns can be created and changed, the versatility of inkjet printing also establishes its value for patterning. Unlike many of the current methods, inkjet printing is not limited to 2D patterns, but can easily be extended to create 3D structures [48].

5. CONCLUSIONS

In conclusion, we have developed an inkjet printing methodology for rapidly creating immobilized concentration gradients of native growth factors on biologically-relevant surfaces that persist for up to 10 days. Since the method is programmable, the gradient shape can be easily changed and overlapping gradients of multiple growth factors and combinatorial arrays can be easily created. This technique has many applications for basic studies in cell biology. Well-characterized concentration gradients of single or multiple growth factors will allow for cell migration studies. The gradients and arrays are also useful for cell proliferation and differentiation studies since a gradient represents a range of concentrations and the overlapping gradients permit the investigation of growth factor combinations at a variety of concentrations printed on the same substrate as demonstrated by the cellular response to the printed combinatorial array of FGF-2 and BMP-2.

ACKNOWLEDGEMENTS

This work was supported partially by Air Force Multidisciplinary University Research Initiative F49620-02-1-0359, National Institute for Occupational Safety and Health/Centers for Disease Control and Prevention 200-2002-00528, the National Science Foundation (Grants No. CTS-0210238 and DMI-9800565), the National Institutes of Health (Grant No. 1 R01 EB00 364-01), the Pennsylvania Infrastructure Technology Alliance (PITA) from the Pennsylvania Department of Community and Economic Development, the Health Resources and Services Administration (Grant No. 1C76 HF 00381-01), the Pittsburgh Tissue Engineering Initiative (JAP), the National Tissue Engineering Center, the Department of Defense, the Scaife Foundation, and the Philip and Marsha Dowd Engineering Seed Fund (EDM). We wish to thank MicroFab Technologies, Inc. for donating inkjets. Thanks to Lawrence Schultz, David Pane, Dr. Jason Smith, Dr. Lauren Ernst, Dr. Frederick Lanni, and Kang Li for technical help and thoughtful discussions.

ABBREVIATIONS

ALP	=	Alkaline phosphatase
2D	=	Two-dimensional
BMP-2	=	Bone morphogenetic protein-2
CS	=	Calf serum
Cy5	=	Cyanine 5
Cy7	=	Cyanine 7
DI	=	Deionized
ECM	=	Extracellular matrix
FGF-2	=	Fibroblast growth factor-2
HEPES	=	4-(2-hydroxyethyl)-1-piperazineethanesulfonic acid
IGF-II	=	Insulin-like growth factor-II
NA	=	Numerical aperture
PBS	=	Phosphate buffered saline
PS	=	Penicillin/streptomycin

REFERENCES

- [1] Campbell, P. G.; Miller, E. D.; Fisher, G. W.; Walker, L. M.; Weiss, L. E. Engineered spatial patterns of FGF-2 immobilized on fibrin direct cell organization. *Biomaterials*, **2005**, *26*(33), 6762-70.
- [2] Miller, E. D.; Fisher, G. W.; Weiss, L. E.; Walker, L. M.; Campbell, P. G. Dose-dependent cell growth in response to concentration modulated patterns of FGF-2 printed on fibrin. *Biomaterials*, **2006**, *27*(10), 2213-21.
- [3] Shing, Y.; Folkman, J.; Sullivan, R.; Butterfield, C.; Murray, J.; Klagsbrun, M. Heparin affinity: purification of a tumor-derived capillary endothelial cell growth factor. *Science*, **1984**, *223*(4642), 1296-9.
- [4] Peng, H.; Sahni, A.; Fay, P.; Bellum, S.; Prudovsky, I.; Maciag, T.; Francis, C. W. Identification of a binding site on human FGF-2 for fibrinogen. *Blood*, **2004**, *103*(6), 2114-20.
- [5] Sahni, A.; Odrjlin, T.; Francis, C. W. Binding of basic fibroblast growth factor to fibrinogen and fibrin. *J. Biol. Chem.*, **1998**, *273*(13), 7554-9.
- [6] Ruppert, R.; Hoffmann, E.; Sebald, W. Human bone morphogenetic protein 2 contains a heparin-binding site which modifies its biological activity. *Eur. J. Biochem.*, **1996**, *237*(1), 295-302.
- [7] Leslie, M. American Society for Cell Biology. Sprayed-on growth factors guide stem cells. *Science*, **2006**, *314*(5807), 1865.
- [8] Phillippi, J. A.; Miller, E.; Weiss, L.; Huard, J.; Waggoner, A.; Campbell, P. Microenvironments engineered by inkjet bioprinting spatially direct adult stem cells towards muscle- and bone-like subpopulations. *Stem Cells*, **2008**, *26*(1), 127-134.
- [9] Li, Q. G.; Blacher, R.; Esch, F.; Congote, L. F. A heparin-binding erythroid cell stimulating factor from fetal bovine serum has the N-terminal sequence of insulin-like growth factor II. *Biochem. Biophys. Res. Commun.*, **1990**, *166*(2), 557-61.
- [10] Wolpert, L. Positional information and the spatial pattern of cellular differentiation. *J. Theor. Biol.*, **1969**, *25*(1), 1-47.
- [11] Tickle, C. Morphogen gradients in vertebrate limb development. *Semin. Cell. Dev. Biol.*, **1999**, *10*(3), 345-51.
- [12] Singer, A. J.; Clark, R. A. Cutaneous wound healing. *N. Engl. J. Med.*, **1999**, *341*(10), 738-46.
- [13] Gerstenfeld, L. C.; Cullinane, D. M.; Barnes, G. L.; Graves, D. T.; Einhorn, T. A. Fracture healing as a post-natal developmental process: molecular, spatial, and temporal aspects of its regulation. *J. Cell. Biochem.*, **2003**, *88*(5), 873-84.
- [14] Barnes, G. L.; Kostenuik, P. J.; Gerstenfeld, L. C.; Einhorn, T. A. Growth factor regulation of fracture repair. *J. Bone. Miner. Res.*, **1999**, *14*(11), 1805-15.
- [15] Akeson, A. L.; Greenberg, J. M.; Cameron, J. E.; Thompson, F. Y.; Brooks, S. K.; Wiginton, D.; Whitsett, J. A. Temporal and spatial regulation of VEGF-A controls vascular patterning in the embryonic lung. *Dev. Biol.*, **2003**, *264*(2), 443-55.
- [16] Ruhrberg, C.; Gerhardt, H.; Golding, M.; Watson, R.; Ioannidou, S.; Fujisawa, H.; Betsholtz, C.; Shima, D. Spatially restricted patterning cues provided by heparin-binding VEGF-A control blood vessel branching morphogenesis. *Genes Dev.*, **2002**, *16*(20), 2684-2698.
- [17] Lindblom, P.; Gerhardt, H.; Liebner, S.; Abramsson, A.; Enge, M.; Hellstrom, M.; Backstrom, G.; Fredriksson, S.; Landegren, U.; Nystrom, H.; Bergstrom, G.; Dejana, E.; Ostman, A.; Lindahl, P.; Betsholtz, C. Endothelial PDGF-B retention is required for proper investment of pericytes in the microvessel wall. *Genes Dev.*, **2003**, *17*(15), 1835-1840.
- [18] Clark, R. A. Fibrin is a many splendored thing. *J. Invest. Dermatol.*, **2003**, *121*(5), xxi-xxii.
- [19] Clark, R. A. Fibrin and wound healing. *Ann. N Y Acad Sci.*, **2001**, *936*, 355-67.
- [20] Kane, R. S.; Takayama, S.; Ostuni, E.; Ingber, D. E.; Whitesides, G. M. Patterning proteins and cells using soft lithography. *Biomaterials*, **1999**, *20*(23-24), 2363-76.
- [21] Mayer, M.; Yang, J.; Gitlin, I.; Gracias, D. H.; Whitesides, G.M. Micropatterned agarose gels for stamping arrays of proteins and gradients of proteins. *Proteomics*, **2004**, *4*, 2366-2376.
- [22] Caelen, I.; Bernard, A.; Juncker, D.; Michel, B.; Heinzelmann, H.; Delamar, E. Formation of gradients of proteins on surfaces with microfluidic networks. *Langmuir*, **2000**, *16*(24), 9125-9130.
- [23] Jiang, X.; Xu, Q.; Dertinger, S.; Stroock, A.; Fu, T.; Whitesides, G. A general method for patterning gradients of biomolecules on surfaces using microfluidic networks. *Anal. Chem.*, **2005**, *77*(8), 2338-2347.
- [24] Gunawan, R. C.; Silvestre, J.; Gaskins, H. R.; Kenis, P. J.; Leckband, D. E. Cell migration and polarity on microfabricated gradients of extracellular matrix proteins. *Langmuir*, **2006**, *22*(9), 4250-8.
- [25] Klebe, R. J. Cytoscribing: a method for micropositioning cells and the construction of two- and three-dimensional synthetic tissues. *Exp. Cell. Res.*, **1988**, *179*(2), 362-73.
- [26] Turcu, F.; Tratsk-Nitz, K.; Thanos, S.; Schuhmann, W.; Heiduschka, P. Ink-jet printing for micropattern generation of laminin for neuronal adhesion. *J. Neurosci. Methods*, **2003**, *131*(1-2), 141-8.
- [27] Watanabe, K.; Miyazaki, T.; Matsuda, R. Growth factor array fabrication using a color ink jet printer. *Zoolog. Sci.*, **2003**, *20*(4), 429-34.
- [28] Gustavsson, P.; Johansson, F.; Kanje, M.; Wallman, L.; Linsmeier, C. E. Neurite guidance on protein micropatterns generated by a piezoelectric microdispenser. *Biomaterials*, **2007**, *28*(6), 1141-51.
- [29] Ilkhanizadeh, S.; Teixeira, A. I.; Hermanson, O. Inkjet printing of macromolecules on hydrogels to steer neural stem cell differentiation. *Biomaterials*, **2007**, *28*(27), 3936-43.
- [30] De Silva, M. N.; Paulsen, J.; Renn, M. J.; Odde, D. J. Two-step cell patterning on planar and complex curved surfaces by precision spraying of polymers. *Biotechnol. Bioeng.*, **2006**, *93*(5), 919-27.
- [31] Ito, Y.; Chen, G.; Imanishi, Y. Micropatterned immobilization of epidermal growth factor to regulate cell function. *Bioconjug. Chem.*, **1998**, *9*(2), 277-82.
- [32] DeLong, S. A.; Moon, J. J.; West, J. L. Covalently immobilized gradients of bFGF on hydrogel scaffolds for directed cell migration. *Biomaterials*, **2005**, *26*(16), 3227-34.
- [33] Mujumdar, R. B.; Ernst, L. A.; Mujumdar, S. R.; Lewis, C. J.; Waggoner, A. S. Cyanine dye labeling reagents: sulfoindocyanine succinimidyl esters. *Bioconjug. Chem.*, **1993**, *4*(2), 105-11.
- [34] Weiss, L. E.; Schultz, L.; Miller, E. D. *Inkjet Deposition System with Computer Vision-Based Calibration for Targeting Accuracy*; CMU-RI-TR-06-15; Carnegie Mellon University: Pittsburgh, March **2006**.
- [35] Gonzalez, R. C.; Woods, R. E.; Eddins, S.L. *Digital Image Processing Using MATLAB*. 1st ed.; Prentice Hall: Upper Saddle River, **2003**.
- [36] Abramoff, M. D.; Magelhaes, P.J.; Ram, S.J. Image processing with Image. *J. Biophotonics Int.*, **2004**, *11*(7), 36-42.
- [37] Campbell, P. G.; Skaar, T. C.; Vega, J. R.; Baumrucker, C. R. Secretion of insulin-like growth factor-I (IGF-I) and IGF-binding proteins from bovine mammary tissue in vitro. *J. Endocrinol.*, **1991**, *128*(2), 219-28.
- [38] Deegan, R. D.; Bakajin, O.; Dupont, T. F.; Huber, G.; Nagel, S. R.; Witten, T. A. Capillary flow as the cause of ring stains from dried liquid drops. *Nature*, **1997**, *389*(23), 827-829.
- [39] Nakamura, M.; Kobayashi, A.; Takagi, F.; Watanabe, A.; Hiruma, Y.; Ohuchi, K.; Iwasaki, Y.; Horie, M.; Morita, I.; Takatani, S. Biocompatible inkjet printing technique for designed seeding of individual living cells. *Tissue Eng.*, **2005**, *11*(11-12), 1658-66.
- [40] Raines, E. W.; Ross, R. Compartmentalization of PDGF on extracellular binding sites dependent on exon-6-encoded sequences. *J. Cell. Biol.*, **1992**, *116*(2), 533-43.
- [41] Besner, G. E.; Whelton, D.; Crissman-Combs, M. A.; Steffen, C. L.; Kim, G. Y.; Brigstock, D. R. Interaction of heparin-binding EGF-like growth factor (HB-EGF) with the epidermal growth factor receptor: modulation by heparin, heparinase, or synthetic heparin-binding HB-EGF fragments. *Growth. Factors*, **1992**, *7*(4), 289-96.
- [42] Rosen, E. M.; Goldberg, I. D.; Kacinski, B. M.; Buckholz, T.; Vinter, D. W. Smooth muscle releases an epithelial cell scatter factor which binds to heparin. *In Vitro Cell Dev. Biol.*, **1989**, *25*(2), 163-73.
- [43] Jackson, R. L.; Busch, S. J.; Cardin, A. D. Glycosaminoglycans: molecular properties, protein interactions, and role in physiological processes. *Physiol. Rev.*, **1991**, *71*(2), 481-539.
- [44] Humphrys, S. T. Design, production and characterization of IGF-I analogues containing heparin-binding domains. PhD Dissertation, University of Adelaide, South Australia, **2000**.
- [45] Upton, Z.; Webb, H.; Hale, K.; Yandell, C. A.; McMurtry, J. P.; Francis, G. L.; Ballard, F. J. Identification of vitronectin as a novel insulin-like growth factor-II binding protein. *Endocrinology*, **1999**, *140*(6), 2928-31.

- [46] Katagiri, T.; Yamaguchi, A.; Komaki, M.; Abe, E.; Takahashi, N.; Ikeda, T.; Rosen, V.; Wozney, J. M.; Fujisawa-Sehara, A.; Suda, T., Bone morphogenetic protein-2 converts the differentiation pathway of C2C12 myoblasts into the osteoblast lineage. *J. Cell. Biol.*, **1994**, *127*(6 Pt 1), 1755-66.
- [47] Nakayama, K.; Tamura, Y.; Suzawa, M.; Harada, S.; Fukumoto, S.; Kato, M.; Miyazono, K.; Rodan, G. A.; Takeuchi, Y.; Fujita, T. Receptor tyrosine kinases inhibit bone morphogenetic protein-Smad responsive promoter activity and differentiation of murine MC3T3-E1 osteoblast-like cells. *J. Bone. Miner. Res.*, **2003**, *18*(5), 827-35.
- [48] Weiss, L.; Amon, C.; Finger, S.; Miller, E.; Romero, D.; Verdinelli, I.; Walker, L.; Campbell, P., Bayesian computer-aided experimental design of heterogeneous scaffolds for tissue engineering. *Comput-Aided Des.*, **2005**, *37*(11), 1127-1139.

Received: August 3, 2007

Revised: October 26, 2007

Accepted: June 24, 2008

Copyright of *Combinatorial Chemistry & High Throughput Screening* is the property of Bentham Science Publishers Ltd. and its content may not be copied or emailed to multiple sites or posted to a listserv without the copyright holder's express written permission. However, users may print, download, or email articles for individual use.